

The velocity field beneath wind-waves — observations and inferences

W.M. Drennan^a, K.K. Kahma^b and M.A. Donelan^a

^a*National Water Research Institute, Canada Centre for Inland Waters, Burlington, Ontario L7R 4A6, Canada*

^b*Finnish Institute of Marine Research, P.O. Box 33, Helsinki, Finland*

(Received 31 July 1991; accepted after revision 15 January 1992)

ABSTRACT

Drennan, W.M., Kahma, K.K. and Donelan, M.A., 1992. The velocity field beneath wind-waves — observations and inferences. *Coastal Eng.*, 18: 111–136.

An extensive set of measurements taken from a fixed tower is used to study the velocity field under wind waves. Velocity measurements, made with miniature drag spheres, are compared with linear theory estimates of the orbital velocities obtained from measured surface elevation. Results are presented in the context of how well linear theory is able to predict wave-induced forces on cylindrical structural members. Linear theory is seen to predict the flow velocities to within about 7%. Furthermore, both the inertial and drag forces are generally well predicted by linear theory, although small scale turbulent motions not accounted for by linear theory can result in significantly higher inertial forces on smaller structural members.

INTRODUCTION

The design of cost-effective offshore structures is highly dependent on an accurate estimation of wave forces which, in turn, depend on the wave orbital velocities, accelerations and pressures. Very few measurements have been made of actual velocities beneath natural wind-generated waves and the design engineer generally relies on linear wave theory to derive appropriate design forces from a suitable climatology of wave (surface elevation) information. Recent results, however, show that the predicted forces can differ from observed ones by as much as 50 to 100% (Ramberg and Niedzwecki, 1979). A large part of this uncertainty is due to inaccuracies in the model by which flow velocities (and thence forces which are related to the square of velocity) are calculated. Although laboratory studies (e.g. Vis, 1980) have generally

Correspondence to: W.M. Drennan, National Water Research Institute, P.O. Box 5050, Canada Centre for Inland Waters, Burlington, Ontario L7R 4A6, Canada.

indicated good agreement between measured and predicted velocities, conditions in the field can differ dramatically from those in the laboratory. In particular, the presence of variable currents and the high local accelerations associated with wave breaking (see Melville and Rapp, 1985) can have important consequences on local velocities and wave forces.

Typically, the forces are predicted using Morison's equation,

$$F_u(t) = C_D \rho r u(t) |u(t)| + C_M \rho \pi r^2 \dot{u}(t) \quad (1)$$

(Morison et al., 1950), which estimates the incremental horizontal force per unit length exerted by a moving fluid on a fixed vertical cylinder. Here, ρ is the fluid density, r is the radius of the cylinder, C_D and C_M are drag and inertial coefficients and $u(t)$ and $\dot{u}(t)$ are horizontal fluid velocity and acceleration. C_D and C_M are functions of the Reynolds number $Re = 2|u|r/\nu$, the relative surface roughness ($k_d/2r$) and the Keulegan-Carpenter number $N_{kc} = AT/2r$, where ν is the fluid kinematic viscosity, k_d is the average roughness diameter, A is the velocity amplitude of the oscillatory part of the flow, and T is its period.

Morison's equation ignores wave drag, which occurs if the cylinder is at or near density interfaces, and skin drag. Nevertheless, for most engineering applications the form drag and inertial resistance modelled by Morison's equation are the dominant forces. Laboratory measurements of the in-line (with horizontal velocity) force on vertical cylinders seem to agree well with that deduced from Morison's equation (Bearman et al., 1985).

The behaviour of the drag and inertial coefficients with Reynolds and Keulegan-Carpenter numbers has been the subject of many investigations (see Sarpkaya and Isaacson, 1981 for a summary), most of which have been carried out in laboratories under idealized conditions of uni-directional, planar oscillatory or circular oscillatory flows. Strong Reynolds number and Keulegan-Carpenter number dependencies on the drag and inertial coefficients imply that the standard practice of using constant values for these coefficients for force calculations over the entire length of vertical cylinders is fraught with error (Ramberg and Niedzwecki, 1979). An additional source of error arises in the calculation of orbital velocities from observed surface elevations using theoretical models. For irregular seas, these models are based on linear theory and one or two ad hoc assumptions. However, a new model by Donegan et al. (1992) has a firmer theoretical foundation and has shown favourable comparisons against laboratory data.

Over the past few decades, several papers have appeared comparing measured field velocities with those predicted by linear theory. Both Guza and Thornton (1980) and Thornton and Krapohl (1974) investigating, respectively, shoaling waves and swell, report good agreement between observed and measured flow velocities — typically to within 10%. Simpson (1969) finds similar results from measurements in 6 metres of water off the end of a

pier, with discrepancies of up to 15% in velocity. There are, however, important differences between two recent works dealing with active wind sea conditions. While both Battjes and van Heteren (1984) and Cavaleri et al. (1978) report fairly good agreement (to within 20%) between measured and predicted velocity magnitudes, Cavaleri, Ewing and Smith report observations indicating that the phase between horizontal and vertical velocity components can be substantially different from that predicted. In particular, under active wind-sea conditions these discrepancies were typically around 30° . Similar results have been observed by Shonting (1970). This phase difference which cannot be explained by linear theory would have, if confirmed, important implications for momentum transport rates in the water column: typically, it implies a momentum transfer many times larger than the momentum input from the wind at the surface.

Although most of the above comparisons are carried out between measured and predicted r.m.s. velocities, from the point of view of structural design it is the peak velocities that are most significant. As the steepest waves tend to be the most nonlinear, the question must be asked as to how well linear theory predicts the peak velocities. Thus, the matter of predicting velocities and wave forces in an active wind-sea is far from settled and it was partly to resolve these issues that the WAVES (Water–Air Vertical Exchange Studies) experiments were carried out (Donelan and Kahma, 1987).

EXPERIMENT

A fixed tower provides the ideal platform for measurements of sub-surface velocities and that of the National Water Research Institute in Lake Ontario is particularly well suited to this purpose. Having been designed expressly for wave measurements, the tower is free of cross-bracing in the vicinity of the water surface (see Fig. 1). The tower is situated 1.1 kilometres offshore in 12.5 metres of water, as indicated in Fig. 2. Power is supplied to the tower via underwater cables and 48 channels of data, sampled at 20 Hz by computer, are transmitted by cable to shore. Further details of the research site are given in Donelan et al. (1985).

The instruments used for measuring both vertical and horizontal components of velocity were “drag spheres”, in which the fluid force on a sphere yields a measure of the velocity components (Donelan and Motycka, 1978). The three drag spheres were mounted on a rotatable mast at nominal depths of 1.2 m, 2 m and 4 m. The mast could be rotated by control from the shore station so that the axes of the drag spheres were aligned normal to the mean wave direction. The instruments thus yielded vertical and horizontal (down-wave) velocity components. The size of the drag spheres (4 mm diameter) was such that they responded essentially to drag and not to inertial effects in the range of wave heights and periods expected (Donelan and Motycka, 1978).

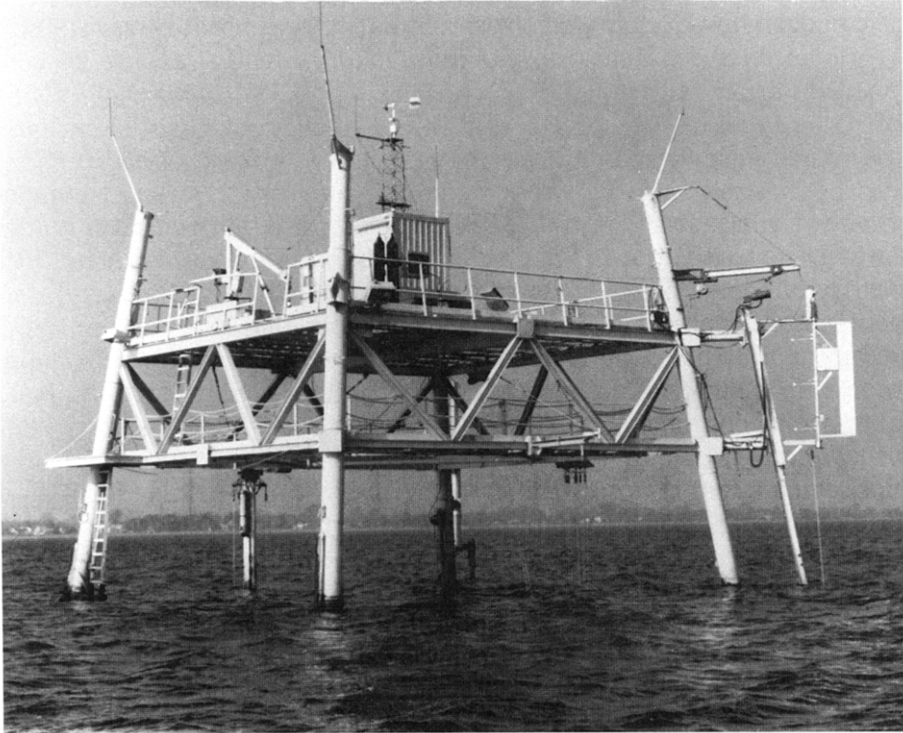


Fig. 1. CCIW tower, Lake Ontario.

Since the drag response is nonlinear (almost perfectly a square law in the Reynolds number range used), the instruments were zeroed mechanically before and after each measurement run by means of pneumatically activated sleeves that shielded the drag spheres from the ambient flows. The drag spheres were carefully calibrated both before and after field exposure. Calibration was accomplished by towing the instruments in the 120 m towing tank of the National Water Research Institute.

In addition to the drag sphere measurements, ten wave staffs were deployed at various locations around the tower to provide wave height information. Of particular interest to this paper is a wave staff located on the mast rotator, about 50 cm from the drag spheres. We also report mean wave directional properties obtained from an array of six wave staffs arranged at the apices and center of a pentagon of 25 cm radius. More detailed wave directional information may be found in Tsanis and Donelan (1989). An anemometer-bivane situated on a mast 12 m above the water surface yielded measurements of wind speed U_{12} and direction (θ_w). Measurements of relative humidity and air and water temperatures were also recorded.

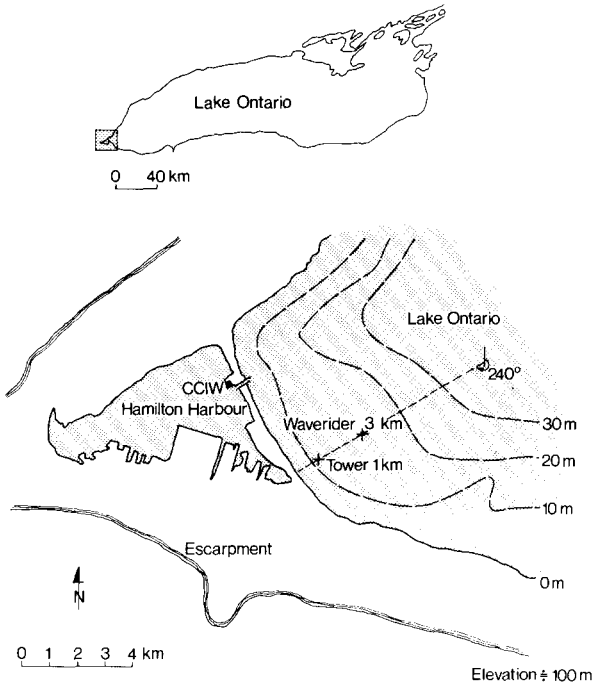


Fig. 2. Map indicating tower location.

ANALYSIS

During the WAVES field season of fall 1985, some forty data runs of forty to eighty minutes duration were made. Processing of the drag sphere and associated wave staff data has consisted of applying spectral analysis using fast Fourier transforms (FFTs) based on blocks of 8192 points (6.83 minutes). This choice of block length permitted interpretation of some of the lower frequency information (to less than 0.01 Hz), while giving enough independent blocks for reliable statistical estimation. To reduce contamination of the low spectral densities through window leakage from the peak, a 4-term Blackman-Harris taper (Harris, 1978) was applied to the individual blocks. Four adjacent spectral estimates were averaged so that each plotted point has 64 degrees of freedom (for the 90 minute runs) corresponding to 95% confidence levels of 1.28 and 0.72. It should be noted that the comparisons with linear theory that follow were not affected by this sampling variability since surface elevation and velocity records were coincident in time and (almost) in space.

The implementation of linear theory was based on surface elevation measurements taken at a wave staff offset 22.5 cm downwave and 45 cm cross-wave from the drag spheres. The water depth d and distance of the drag sphere

below the surface z were based on the mean water level during the run. The surface elevation signals were Fourier transformed as described above so as to calculate the Fourier coefficients. The wave number k associated with each frequency f was then calculated from linear theory, along with the quantities

$$T_{\eta u} = 2\pi f \frac{\cosh(k(d-z))}{\sinh(kd)} e^{i\phi_{\eta u}} \quad \text{and} \quad T_{\eta w} = 2\pi f \frac{\cosh(k(d-z))}{\cosh(kd)} e^{i\phi_{\eta w}} \quad (2)$$

which represent the transfer functions between the surface elevation η and velocities u and w , respectively. The quantity $\phi_{\eta u}$ corrects for the phase shift (with frequency) due to the downwave spatial offset between the wave staff and drag spheres, along with that induced by sampling and electronic filtration. Finally, the linear theory velocity estimates u_l and w_l were determined by inverse Fourier transform. We note here that unidirectional long-crested waves were assumed with the result that u_l and w_l are 90° out of phase. We emphasize that the correction $\phi_{\eta u}$ is applied to the linear theory velocity estimates; the measured velocities are not altered in any way.

For determining the directional spectra, data collected from each of the six wave staffs of the array were averaged down to 4 Hz, and cross spectra were calculated based on blocks of 1024 points. A maximum likelihood method (MLM) based on Jefferys (1986) with 10 degree directional spacing was employed. Only selected results from the directional analysis will be presented here; more detailed results are available in Tsanis and Donelan (1989).

RESULTS

Data summary

In Table 1, we summarize results for some fifteen runs for which a linear analysis was carried out. Of these, we have selected four runs for detailed presentation: 85105, 85111, 85145 and 85159. This subset was selected so as to represent a good cross-section of the conditions encountered. The prevailing winds in the area are from the southwest and, for these cases, the fetch at the tower is of the order of one to two kilometres. Storms tracking south of Lake Ontario often result in winds from the east, and for these cases the fetch at the tower is of the order of 200 to 300 kilometres. Consequently, a classification of the runs by wind direction is essentially a classification by wave development: waves from the west are fetch limited, with a corresponding low wave age (U_{12}/c_p , where c_p is the phase velocity at the peak frequency, is the inverse wave age) while those from the east tend to be older or more developed. 85111 represents an overdeveloped sea ($U_{12}/c_p = 0.1$) with swell propagating eastward along the major axis of Lake Ontario; 85105 ($U_{12}/c_p = 0.9$), nearly fully developed waves from the east; 85145 ($U_{12}/c_p = 1.3$), an underdeveloped east wind case; and 85159 ($U_{12}/c_p = 4.2$), with very under-

TABLE 1

WAVES 85 — drag sphere results

Run No.	U_{12} (m/s)	θ_w (°)	D (°)	H_s (cm)	f_p (Hz)	U/c_p	depth (cm)	σ_u (cm/s)	σ_w (cm/s)	G_u	G_w	ϕ_{uw} (°)
85104	6.7	63	70	50	0.30	1.3	146	12.8	13.3	1.05	1.14	92
							186	11.5	10.2	1.24	0.98	97
							386	6.2	6.1	1.8	1.7	
85105	10.5	87	75	187	0.14	0.9	158	43.9	38.1	0.94	0.91	91
							198	44.3	33.6	1.08	0.98	98
							398	35.0	25.3	1.11	1.01	92
85107	7.1	100	75	189	0.14	0.6	159	44.9	41.1	0.80	0.93	92
							399	36.0	27.4	0.87	0.97	97
85111	0.9	var	55	73	0.20	0.1	151	19.9	19.2	1.07	1.07	89
85116	10.7	250	220	27	0.52	3.6	139	2.2	4.5	0.25	1.07	95
85117	10.4	250	220	26	0.53	3.5	140	3.7	3.9	1.10	1.23	97
85119	8.3	248	265	13	0.52	2.8	139	1.9	2.1	1.08	1.31	97
85125	17.2	90	80	203	0.17	1.9	164	40.4	44.8	0.70	1.01	89
85129	5.2	337		113	0.14	0.5	145	23.7	26.9	0.58	0.95	86
85135	8.0	112	75	62	0.30	1.5	120	17.1	17.8	0.88	0.95	89
							390	7.0	7.5	1.17	1.37	
85140	4.7	13	75	130	0.15	0.5	120	35.3	31.6	1.07	1.04	90
							190	33.3	26.0	1.22	0.95	90
							390	26.0	20.2	1.28	1.25	
85144	14.2	64	75	240	0.14	1.3	132	59.7	51.8	0.90	0.89	93
							202	60.6	45.2	1.10	0.88	93
85145	14.0	67	85	231	0.14	1.3	131	56.9	50.1	0.90	0.92	91
							201	56.0	43.2	1.06	0.89	92
							401	45.4	31.6	1.09	0.97	95
85159	16.0	234	240	49	0.41	4.2	104	15.2	15.0	1.08	1.07	88
							174	9.4	9.3	1.10	1.13	85
							401	4.9	4.2	1.90	1.95	
85160	12.7	230	225	32	0.48	3.9	100	9.2	9.3	1.11	1.15	94
							170	5.0	5.1	1.29	1.37	96

U_{12} , θ_w — wind speed and direction at 12 m; D — wave direction; H_s — $4 \times$ r.m.s. wave height; f_p — frequency of wave peak; U/c_p — wave age; ϕ_{uw} — phase angle between u and w at f_p ; G_u , G_w — variance gain, measured vs. linear theory; σ_u , σ_w — measured r.m.s. of u , w .

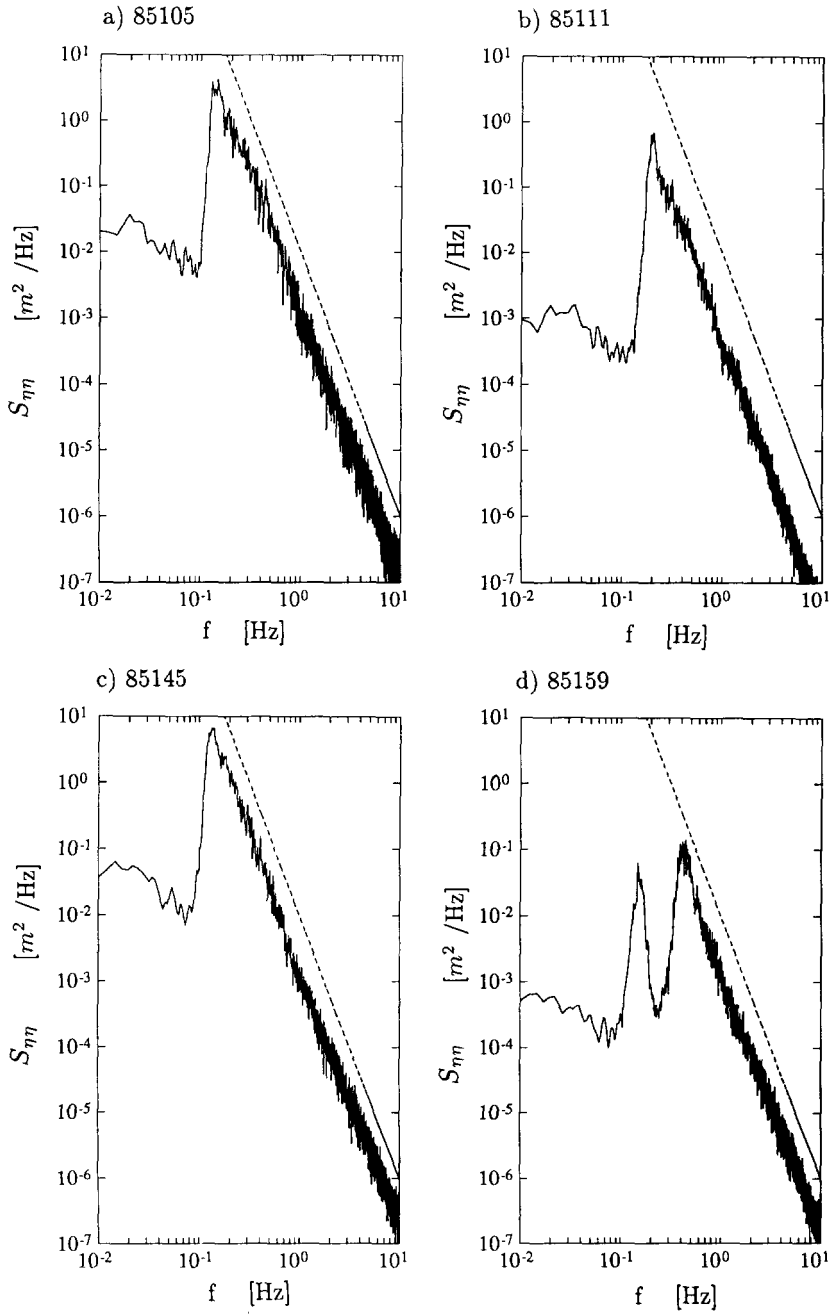


Fig. 3. Wave height spectra $S_{\eta\eta}$, showing f^{-4} reference (---).

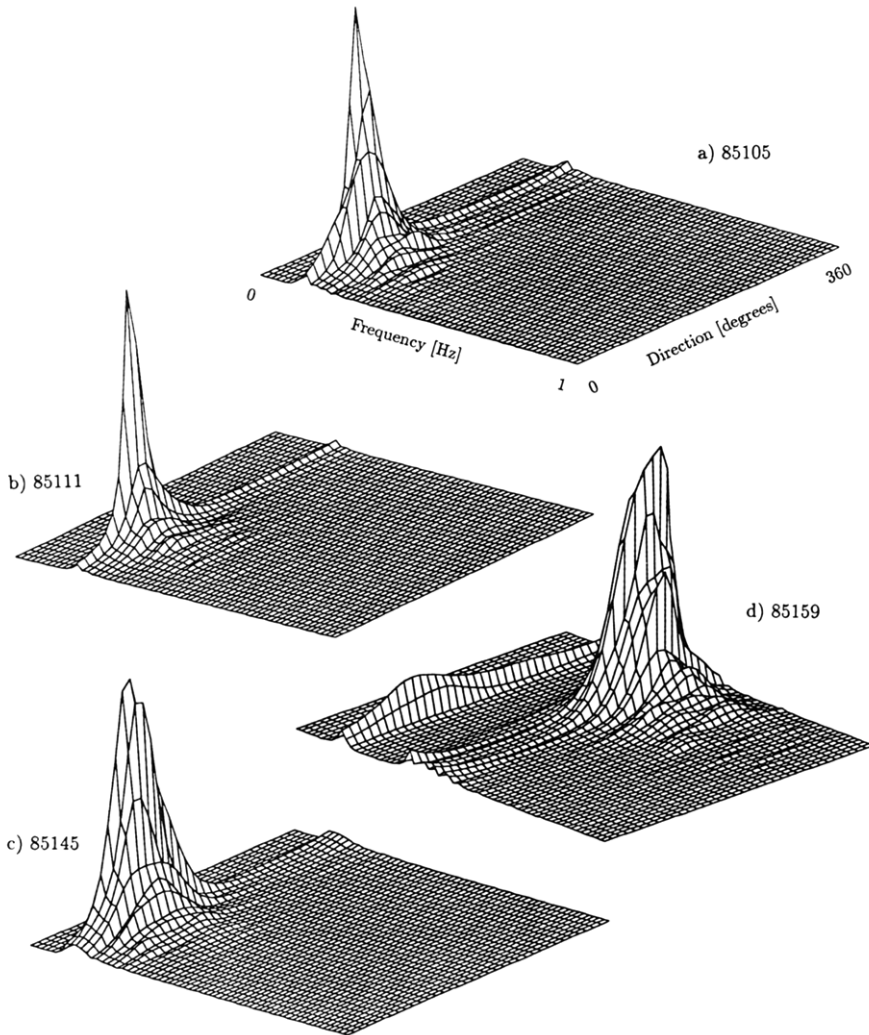


Fig. 4. Directional spectra.

developed (strongly forced) waves from the west. The strongly forced, fetch-limited waves of 85159 are akin to the steep duration-limited waves associated with the outbreak of a storm. In Figures 3 and 4, we show wave height and directional spectra for each of the four cases. Above the peak, the wave height spectra conform to a f^{-4} power law (Donelan et al., 1985). The three east wind cases show waves with frequencies near the spectral peak to be arriving from approximately 70° , which is the principal axis of Lake Ontario. Although the waves in 85159 are predominantly from the west (220°), there is also evidence of 6 second swell from the east.

Wave velocities

In Figs. 5 and 6, we present spectra of the vertical velocity components as measured by the drag sphere, compared with those calculated according to linear theory; sections of the time series are also plotted (Fig. 7). Agreement with linear theory is very good around the peak of the wave spectrum. Away from the peak (and several decades lower in spectral density) the deviations are caused by turbulence generated by the wind-driven sheared current and by wave breaking (Kitaigorodskii et al., 1983). Note that the high frequency regions of the spectra (85105, 85111 and 85159) display slopes of $-5/3$, corresponding to the inertial subrange of isotropic turbulence. For purposes of calculating wave-induced forces on structures, these differences are less important than those occurring around the peak at substantially higher energy levels.

The twelfth column of Table 1, which shows the ratio of the variances (i.e. the integrated velocity spectra) of w and w_l (G_w), provides a measure of how well the velocities are predicted by linear theory. Typically, G_w falls between 0.88 and 1.15, which corresponds to measured velocities within 7% of linear theory predictions. Note that, according to Fig. 8, the larger ratio value for run 85119 is due to an underestimation of the swell component which, in this run, is comparatively large; again, the wind sea is well predicted by linear theory. Exceptions to this are runs 85104 (386 cm depth), 85135 (390 cm), 85140 (390 cm), 85159 (401 cm) and 85160 (170 cm), where the measurements are taken at relatively large depths with low significant wave height. For these cases, the ratio of variances G_w reaches as high as two. This is a result of very low wave energy at the depths of measurement: the drag sphere is out of its operating range. Consequently, the measurements in these cases are spurious. Omitting these obvious outliers, the mean and standard deviation of G_w are 1.02 and 0.11 respectively, so that in 90% of the cases the rms measured velocities are within 9% of theory.

In the case of horizontal velocity, linear theory again is seen to perform well (Fig. 9), although there appear to be deviations at frequencies just above the peak, where linear theory is seen to overpredict the velocity. This phenomenon was previously observed by Forristall et al. (1978), who attributed it to flow nonlinearities. As pointed out by Battjes and van Heteren (1984), however, nonlinearities would tend to have the opposite effect. We attribute the overprediction to the increasing directional spread of the wind sea above the peak (see below): linear theory estimates are based on unidirectional waves, and hence ignore the effects of spreading. In several cases (e.g. 85116) the horizontal velocities appear to be very poorly predicted by linear theory. For run 85116 $G_u = 0.25$, whereas $G_w = 1.07$. As a rule efforts were made to ensure that the drag spheres were aligned normal to the wave direction so that the measured horizontal velocity would correspond to that of the principal

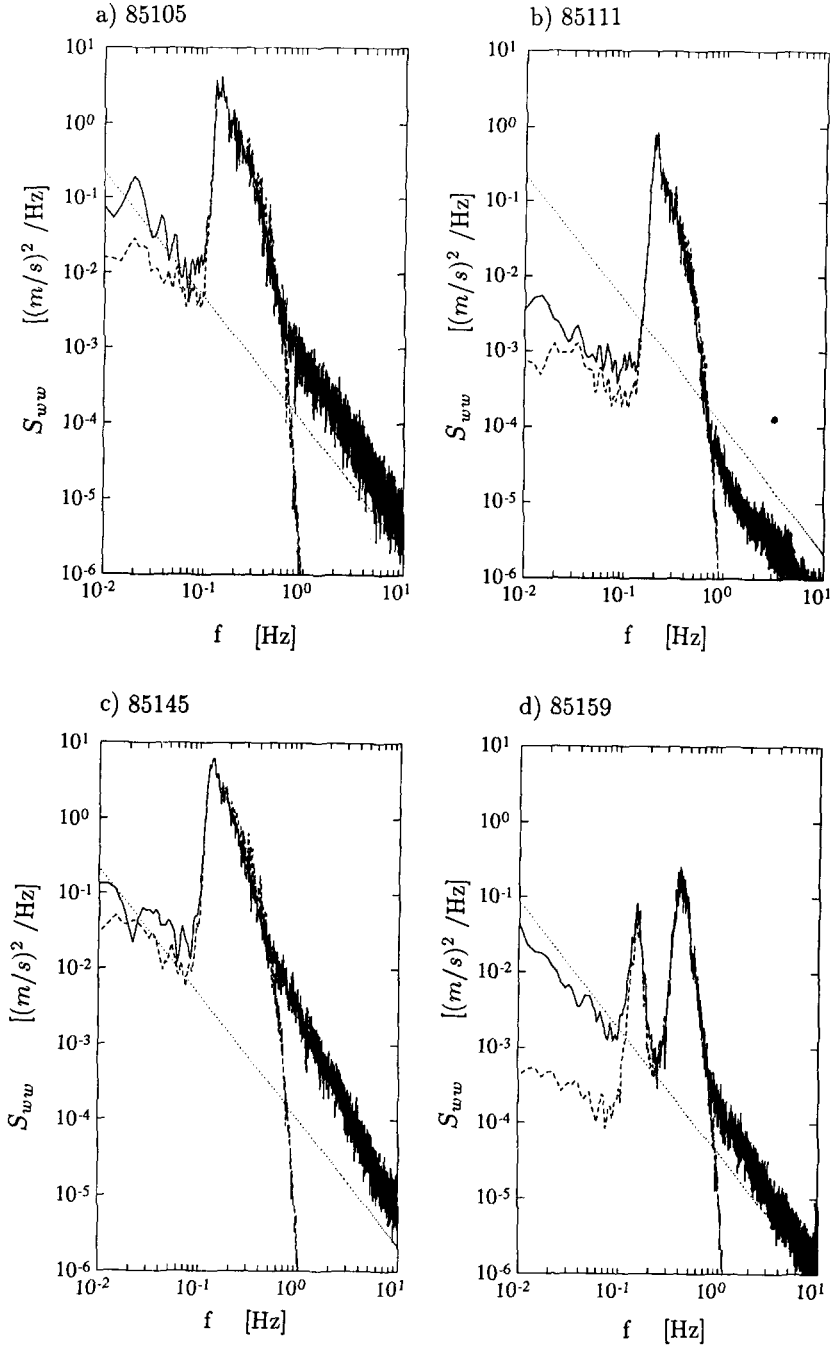


Fig. 5. Vertical velocity spectra, S_{ww} measured (—) and via linear theory (---), showing $f^{-5/3}$ reference slope (.....).

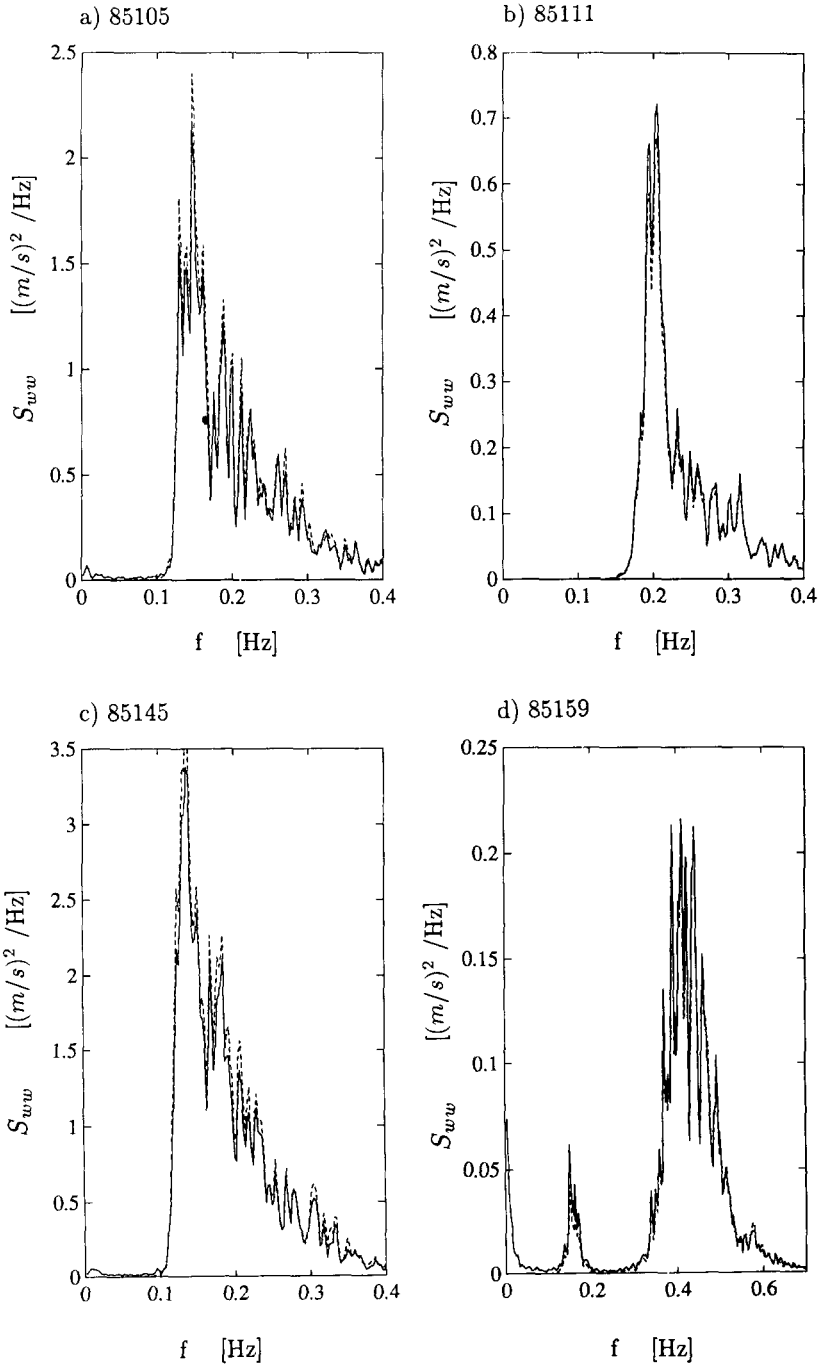


Fig. 6. Vertical velocity spectra, S_{ww} , measured (—) and via linear theory (---).

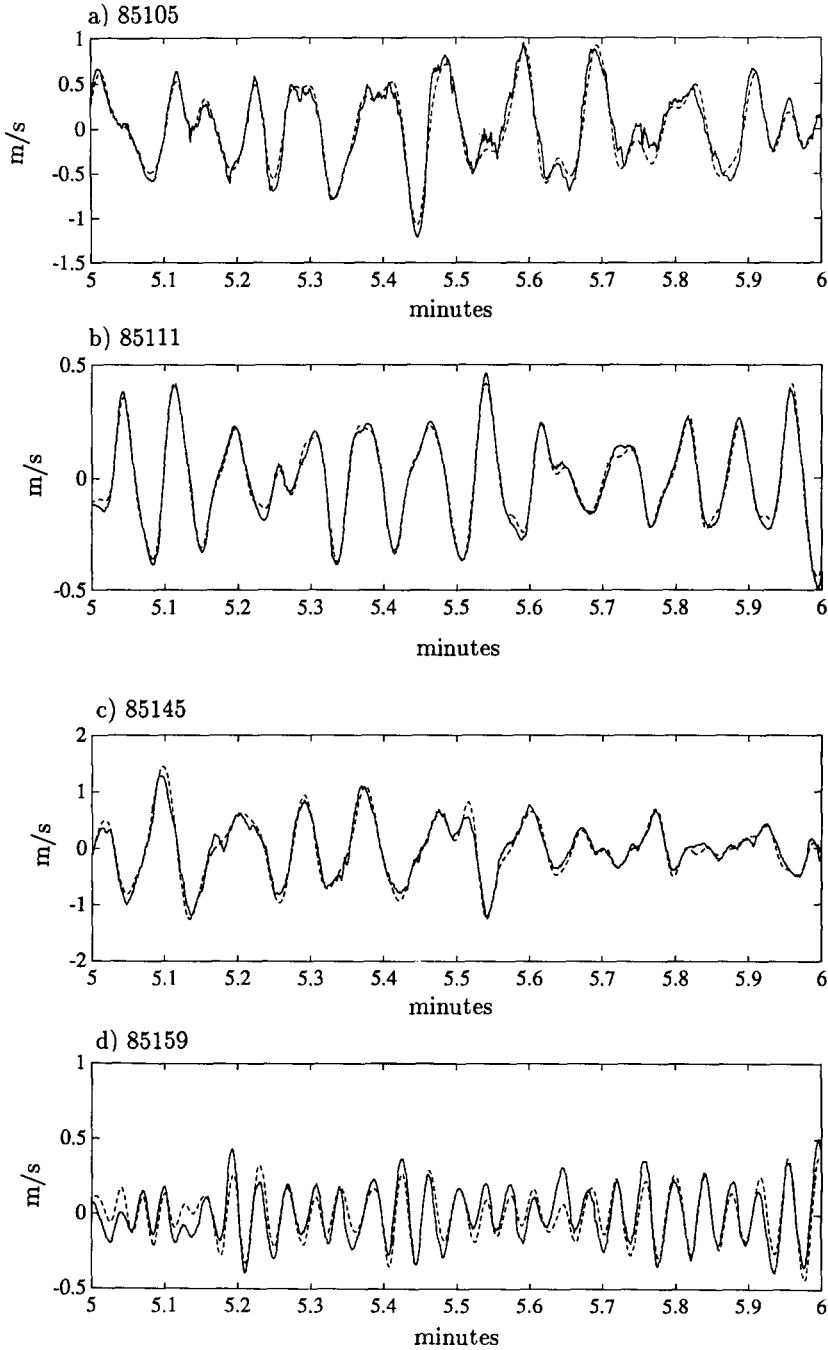


Fig. 7. Time series of vertical velocity w , measured (—) and via linear theory (---).

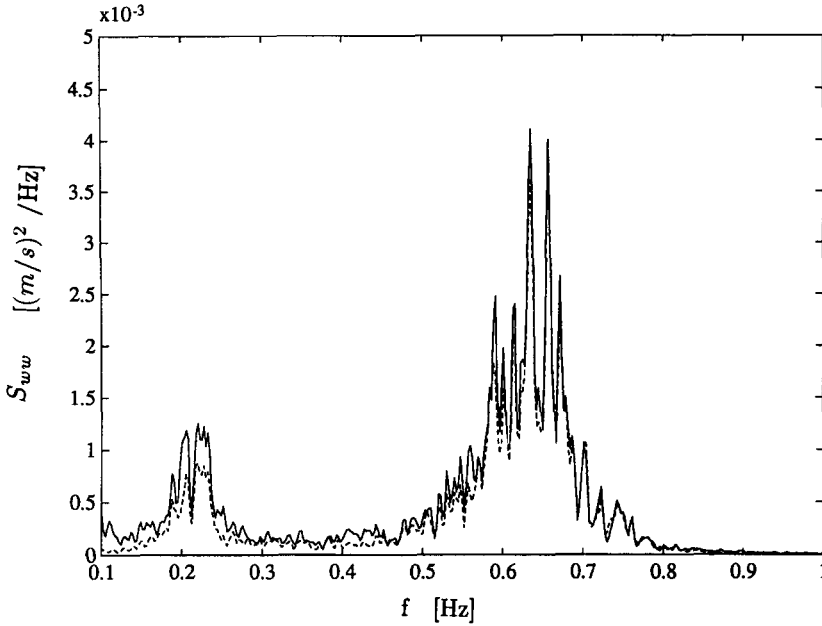


Fig. 8. Vertical velocity spectrum S_{ww} for run 85119, measured (—) and via linear theory (---).

wave direction. For some runs, however, this was not achieved, resulting in the low G_u ratios observed.

As noted above, the directional spread of the wind sea was not taken into account in the linear theory calculations. This can be rectified by computing the horizontal velocities from the full directional spectrum following Donelan et al. (1985):

$$F(f, \theta) = \frac{1}{2} S_{\eta\eta}(f) \beta \operatorname{sech}^2 \beta \{ \theta - \bar{\theta}(f) \} \quad (3)$$

where θ is the wave direction, $\bar{\theta}$ the mean wave direction and

$$\beta = 2.61 (f/f_p)^{+1.3} \quad \text{for } 0.56 < f/f_p < 0.95$$

$$\beta = 2.28 (f/f_p)^{-1.3} \quad \text{for } 0.95 < f/f_p < 1.6$$

$$\beta = 1.24 \quad \text{otherwise}$$

where f_p refers to the peak frequency. To be consistent with linear theory, θ was taken to be the mean wave direction at the wave peak, $\bar{\theta}_p$. The directional wave height spectra were then used to generate the corrected linear horizontal velocity spectra, which are plotted using dotted curves in Figures 9a and d.

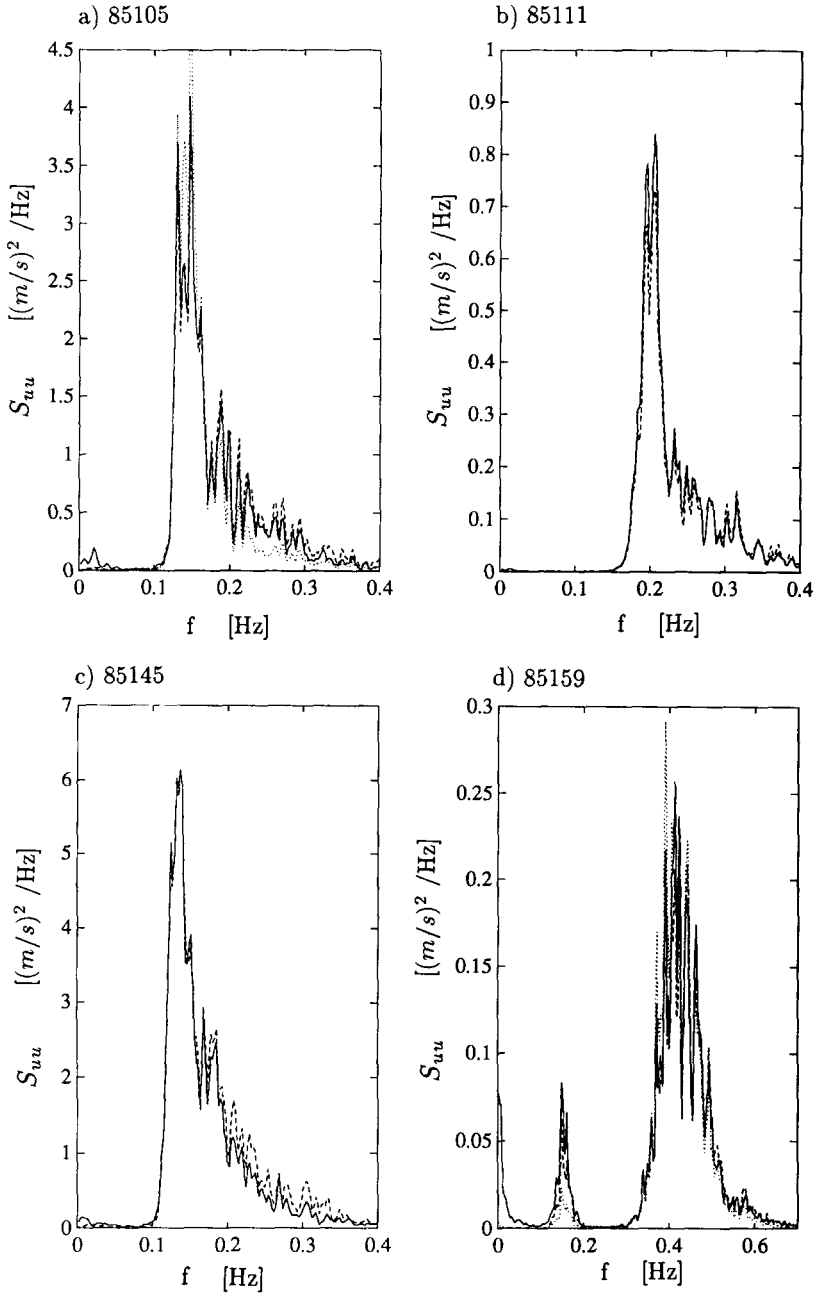


Fig. 9. Horizontal velocity spectra, S_{uu} , measured (—) and via linear theory (---). Corrected for directional spreading (.....).

Directional effects are seen to account for the overprediction of horizontal velocities by linear theory at frequencies about twice the peak.

In Table 1 (last column) we present the phase angle ϕ_{uw} between the horizontal and vertical velocity components as measured by the drag sphere. ϕ_{uw} is calculated from the cospectrum of the two time series and the single value reported is that found by averaging phase angle values for frequencies around the peak, where the coherence between the two signals was greater than 0.95. For the four selected runs, the phase angle (along with 95% confidence limits calculated according to Bendat and Piersol, 1971) and coherence γ^2 are plotted, for frequencies around the peak, in Figs. 10 and 11.

Although linear theory predicts a phase difference between u and w of exactly 90° , experimental results have not always supported this. In particular, Cavaleri et al. (1978) and Cavaleri and Zecchetto (1987) have reported consistent deviations from linear theory of as high as 30° , with current meter measurements taken in active wind sea conditions from a tower in the Adriatic Sea; measurements taken in swell showed the expected phase lag of close to 90° . These results, if correct, would have important implications in the momentum balance, implying a surface flux considerably greater than that derived from wind input at the surface. Our results, taken over a wide range of meteorological conditions do not, however, corroborate these findings. On the contrary, our results support those of Battjes and van Heteren (1984), among others, in finding ϕ_{uw} to be consistent with linear theory predictions. It should be noted that reflected waves from nearby structures or topography can have a strong effect on the measured phase angle.

The paragraphs above indicate that linear theory is generally adequate for estimating the velocity field in a spectral sense. The question remains as to how well linear theory predicts the extreme waves of any event. In order to determine this, joint frequency distributions of u and u_l and of w and w_l were calculated for each of the runs. The corresponding plots for the four selected runs appear in Figure 12, where we have normalized u and u_l by $(\overline{u^2})^{1/2}$ and w and w_l by $(\overline{w^2})^{1/2}$. Also the mean flow (i.e. any current) has been subtracted from the measured velocities and all signals detrended. In the plots, curves of high aspect ratio, centred around the 45° line indicate that linear theory predicts the velocities on a wave by wave basis very well. In general, our data is seen to support this hypothesis although the contours for run 85159 display significantly lower aspect ratios. Recall that this is a west wind case which implies short crested, high frequency waves. In such conditions, the 50 cm horizontal separation between the drag spheres and wave staff (from which the linear theory velocity estimates are calculated) will induce an error visible in wave-by-wave comparisons in that the two instruments will not always see the same wave. This is evident both in the time series plots (Fig. 7d) and in the broadening of the contours in the joint frequency distribution plots.

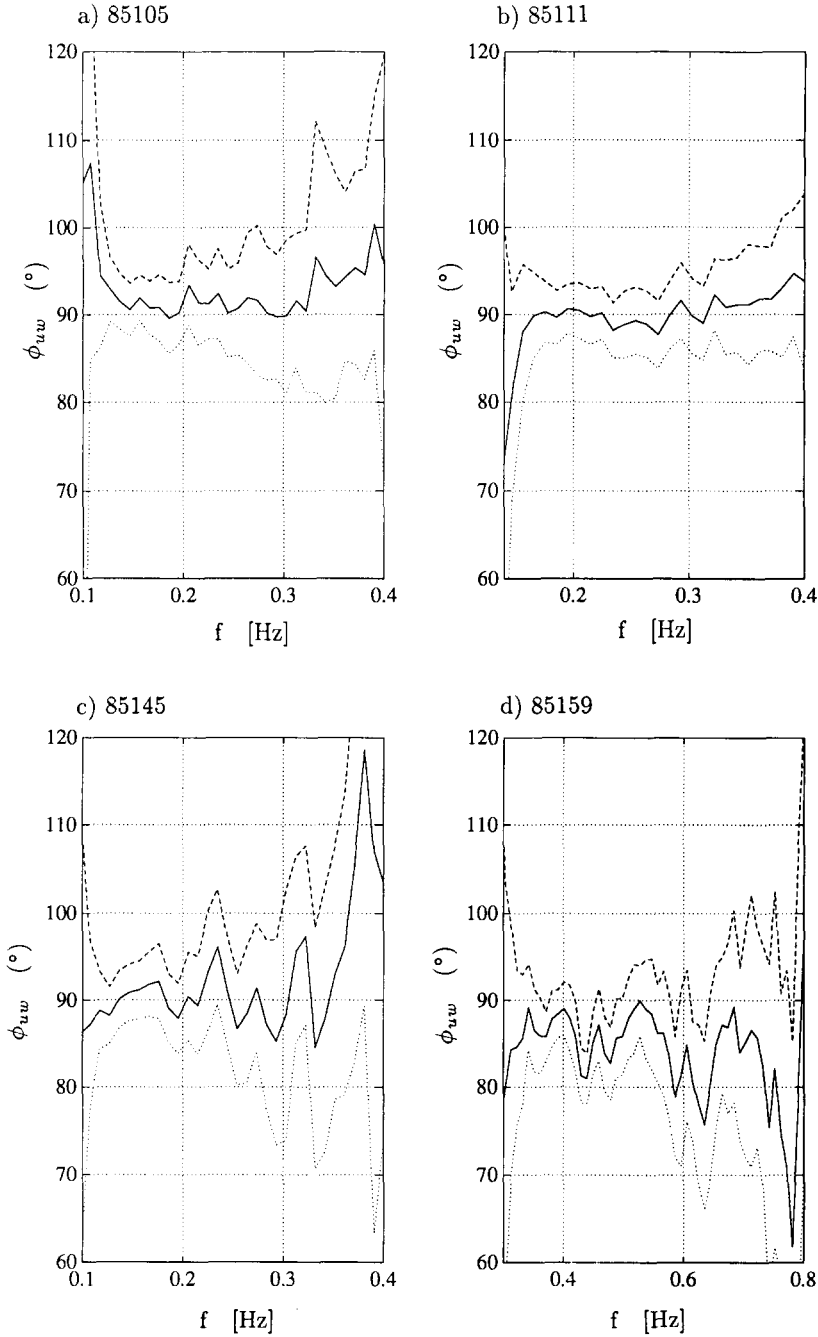


Fig. 10. Phase angle between horizontal and vertical velocities, ϕ_{uw} .

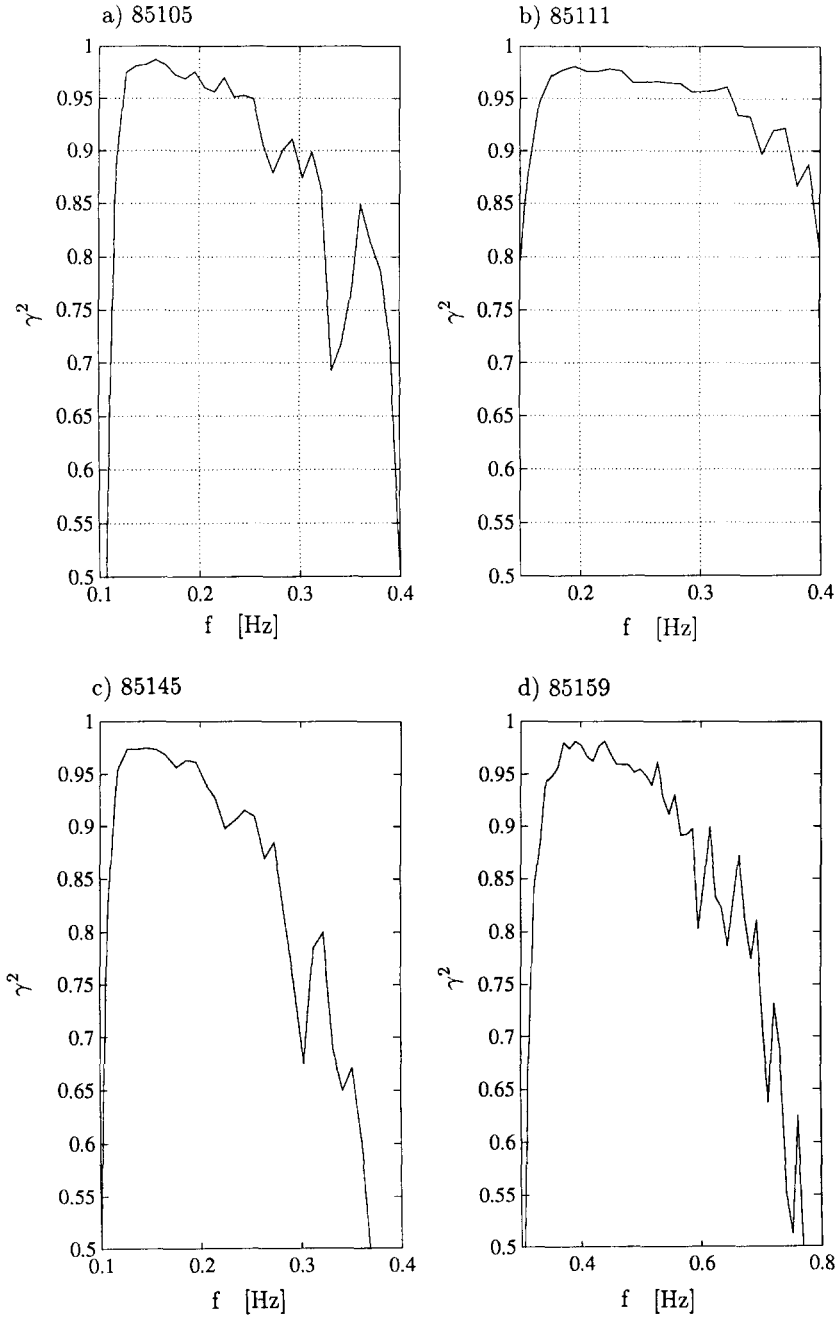
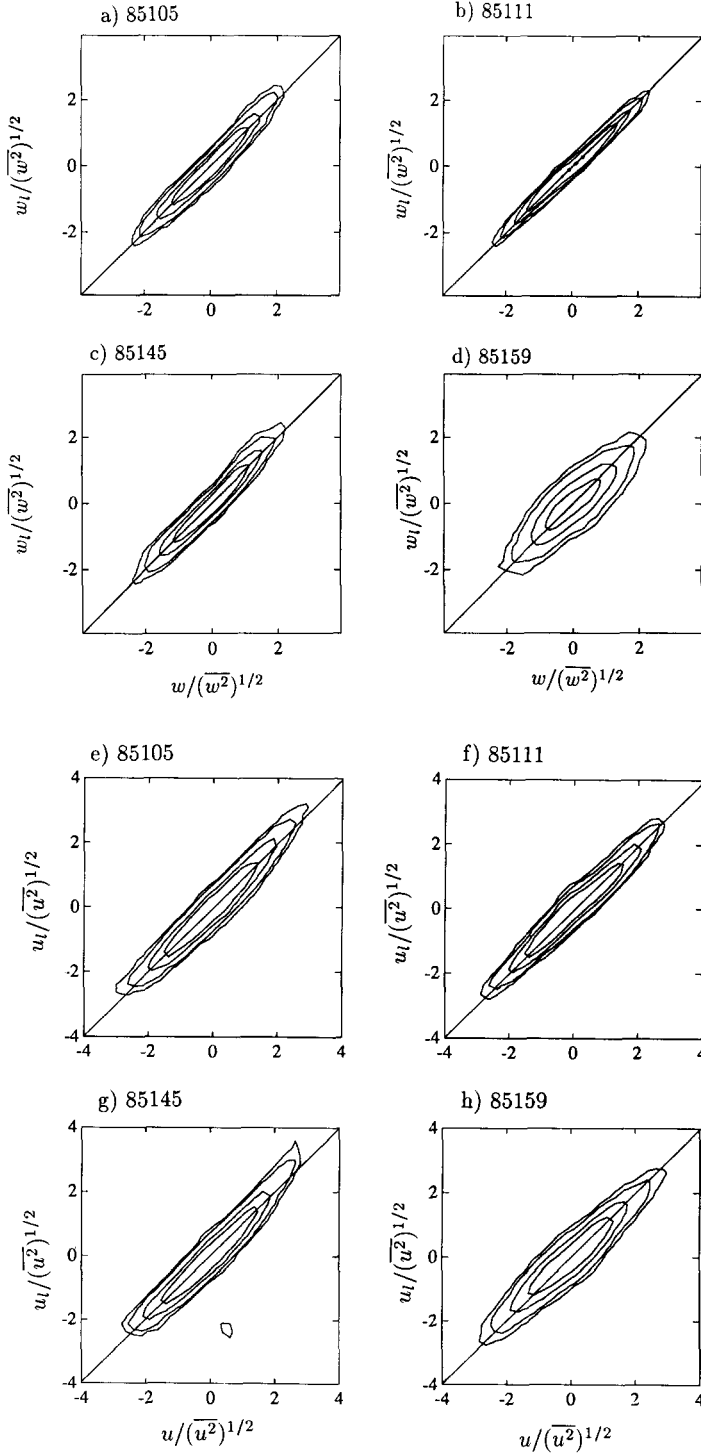


Fig. 11. Coherence between horizontal and vertical velocities, γ^2 .

Fig. 12. Joint frequency distributions of u and u_t , w and w_t .



Wave forces

As pointed out above, wave forces on a vertical cylinder are typically estimated using Morison's equation (1), which requires knowledge of the flow field. This knowledge is often derived from wave height measurements by means of linear (or some other) theory as described above in Section 3. In this section, we compare the force estimates derived from linear theory to those based on drag sphere measurements. In particular, we examine the quantities $u|u|$ and \dot{u} — for convenience, we refer to these as the drag and inertial forces respectively. In Figs. 13 and 14 examples of time series of $u|u|$ and \dot{u} for the four selected runs are given; linear theory estimates are also shown. The time series segments chosen are coincident with those of Fig. 7. We note here that during these runs, the drag spheres were aligned such that the measured horizontal velocity is down-wave and therefore comparable to linear theory velocities. Furthermore, directional spreading of the wind waves was taken into account following Donelan et al. (1985) — see above. The wave-by-wave comparisons of the drag force (Figure 13) show some discrepancies at both larger crests and troughs, but do not indicate any consistent over- or under-prediction.

Figure 15 illustrates the joint frequency distributions of the measured and predicted drag force, $u|u|$ and $u_l|u_l|$ for the four runs. It is evident that the distributions generally follow the 45° line, indicating good agreement between measured and predicted values, but that linear theory has a tendency to overpredict the larger forces under crests and to underpredict the larger forces under troughs (note the curvature in the contours, especially that of Fig. 15a or c). While similar curvature in a joint probability distribution may result from nonzero mean current, this is not the source of the curvature in Fig. 15, because the mean has been subtracted from the velocities to avoid these distortions in the comparison. The deviation is likely related to the use of linear wave theory to model a finite amplitude wave field.

A comparison (Fig. 14) of the measured and predicted inertial forces, \dot{u} and \dot{u}_l , shows clearly the effects of the high frequency turbulence on the measured velocity signal. While the force predicted by linear theory is smoothly varying with time, the measured forces are seen to exhibit significant small scale fluctuations due to the passage of turbulent eddies past the drag sphere. Consequently, the measured local inertial forces are as high as twice those predicted by linear theory! We do note, however, that the linear term \dot{u}_l does predict the observations very well on a larger scale — that is, ignoring the turbulent local accelerations. The typical scale of these high local accelerations is of order 10 cm and they may therefore become significant for small structural members having a diameter about 5 cm.

It is thus seen that there are discrepancies between linear theory and measurements for both the drag and (especially) inertial forces. However, it is

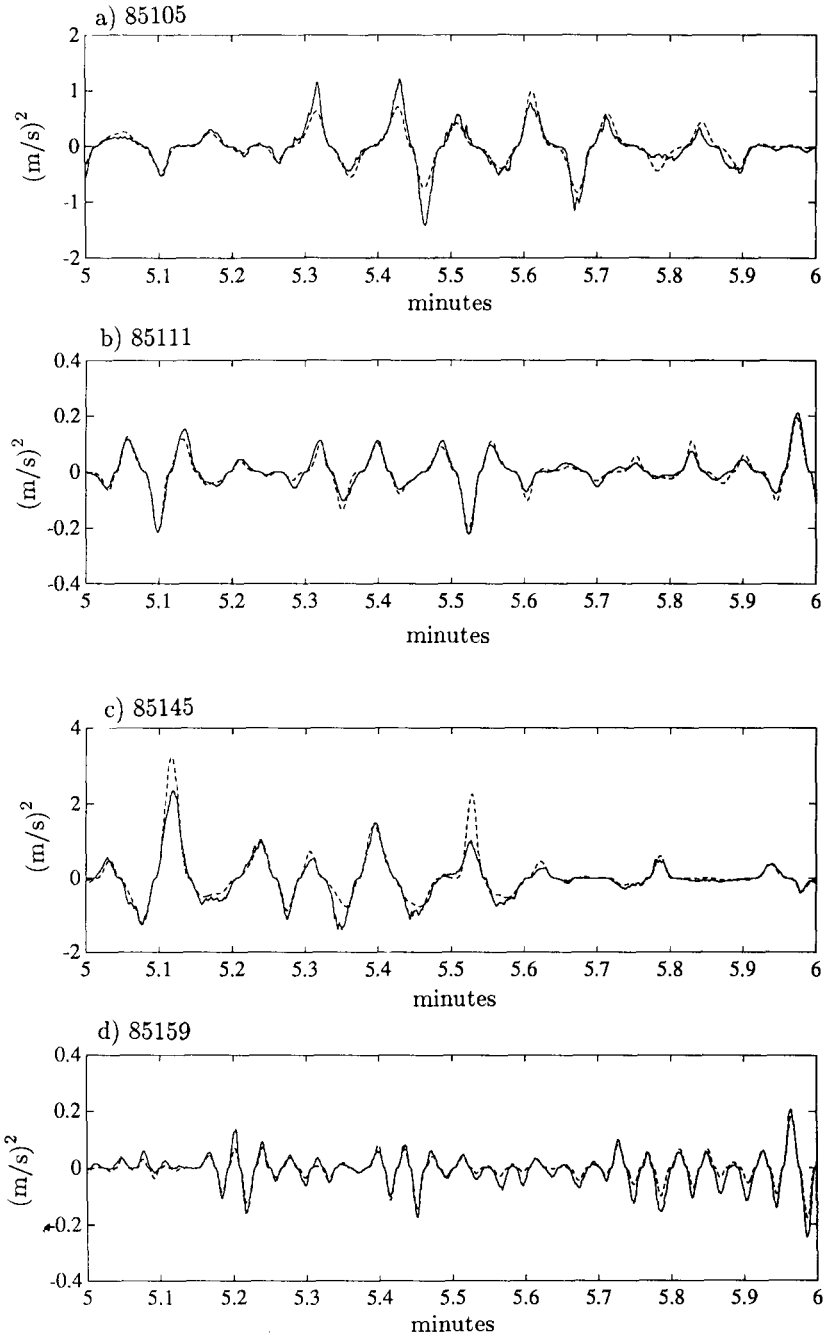


Fig. 13. Time series of $u|u|$ (—) and $u_I|u_I|$ (---).

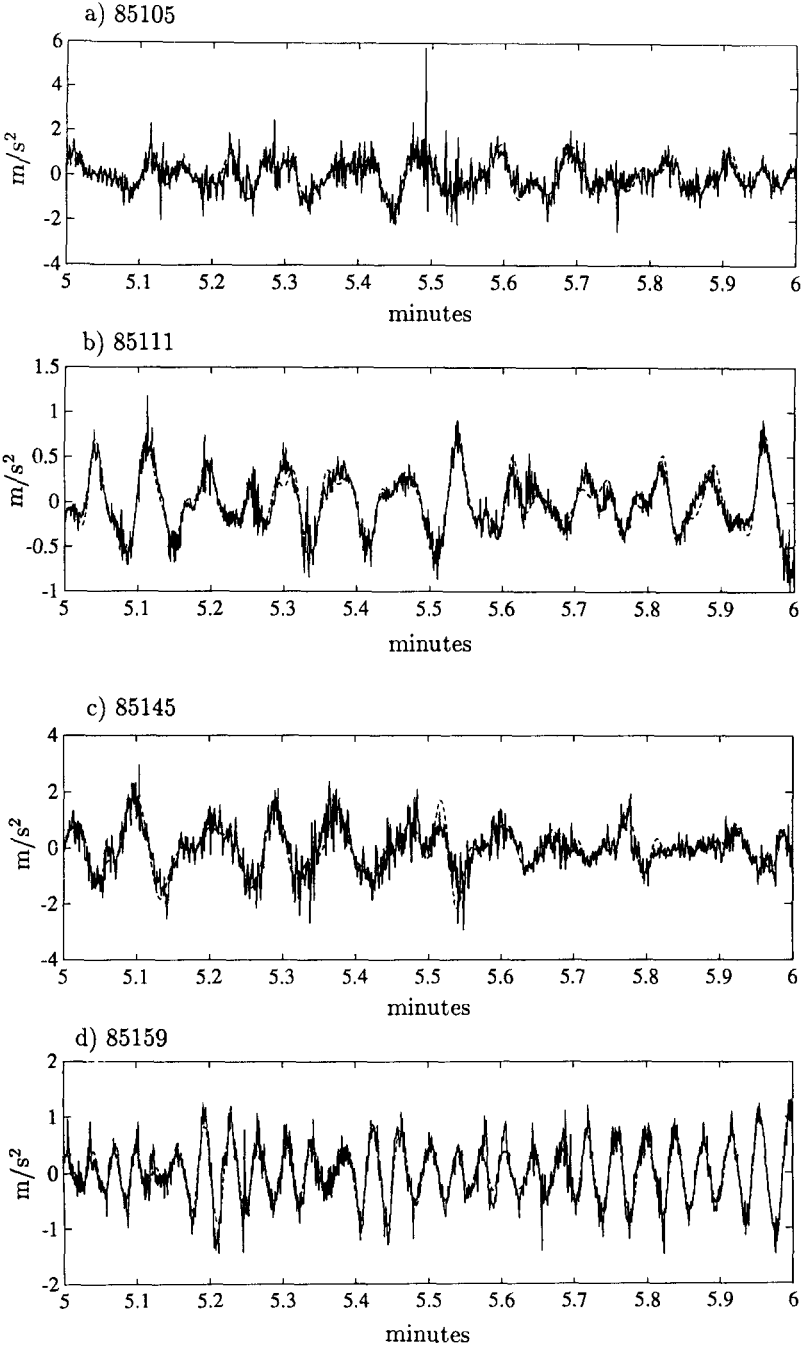


Fig. 14. Time series of \dot{u} (—) and \dot{u}_i (---).

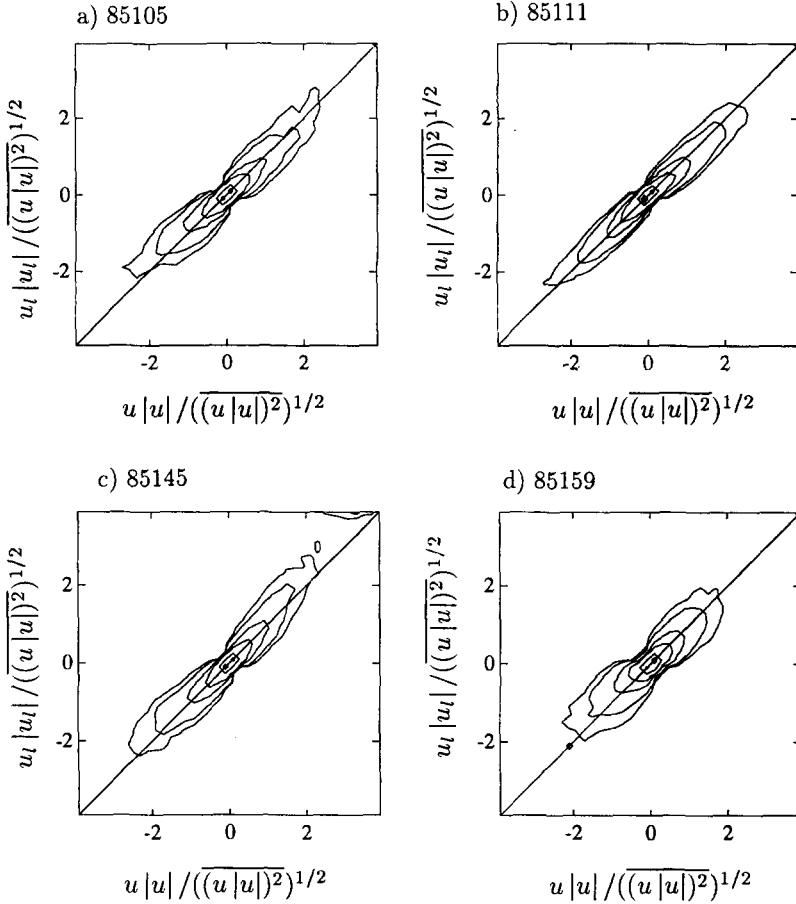


Fig. 15. Joint frequency distributions of $u|u|$ and $u_i|u_i|$.

important to note that these force terms are implemented in Morison's equation with empirically calibrated coefficients. That is, the drag and inertial coefficients C_D and C_M are typically found through laboratory experiments in which a cylinder is subjected to a series of waves (see Sarpkaya and Isaacson, 1981). The forces on the cylinder are usually measured with strain gauges, with the flow velocities being determined from the measured surface elevation using linear theory. Consequently, the differences between linear theory and measured forces, as noted above, are to some degree taken into account through the empirical determination of the force coefficients for the conditions of the laboratory tests. It is therefore very important that the drag and inertial coefficients C_D and C_M used be determined under similar conditions to those of the intended application. Furthermore, as we have seen, the degree of deviation of the measured velocities from linear theory depends on the

degree of wind forcing. Thus the accuracy of C_D and C_M will depend also on wind forcing and other causes of nonlinearity in the wave field.

CONCLUSIONS

The data collected during the WAVES experiments, covering a wide range of meteorological conditions, indicate that linear theory, based on wave height data, is able to predict flow velocities to within about 7%. The agreement between measured and predicted spectral values is very good in the vicinity of the peak of the spectrum, with discrepancies observed at higher frequencies. However, as these discrepancies, resulting from turbulence in the wave field, occur at energy levels one to two orders of magnitude below the peak values their effect on the velocity comparison is minimal. With respect to horizontal velocities in wind-driven seas, it was found that a correction for directional spreading should be applied to the wave height spectrum prior to the implementation of linear theory; otherwise, there is some evidence that the energy at frequencies just above the peak will be overestimated.

Strong evidence was found indicating that the phase angle between horizontal and vertical velocities is very nearly 90° , as indicated by linear theory.

The drag forces $u|u|$ are quite well predicted by linear theory, although larger trough forces tend to be underestimated and crest forces overestimated due to the effects of finite wave height. The inertial forces are somewhat less well predicted due to the effects of high local turbulent accelerations which are not accounted for by linear theory — these are particularly significant for small structural members. Such effects vary with local conditions and may to some extent be offset by the use of drag and inertial coefficients that have been determined under similar conditions. We note here that currents have not been taken into account in the analysis, with the measured velocities being detrended. It is, however, important to note that currents will affect the underlying velocity field — particularly the horizontal velocities — and should be added to the velocities deduced from the wave heights. In particular, they will have a direct impact on the loading on a structure. Whether or not the incremental forces due to currents are large compared with the loadings associated with extreme wave crests will depend on particular conditions.

ACKNOWLEDGEMENTS

Many members of the staff of the National Water Research Institute contributed to this study. We acknowledge, in particular, D. Beesley and R. Desrosiers. This experiment was supported in part by the Panel on Energy Research and Development under PERD project number 62123. K.K. Kahma

and W.M. Drennan would like to thank the National Water Research Institute for its hospitality while this work was carried out.

REFERENCES

- Battjes, J.A. and van Heteren, J., 1984. Verification of linear theory for particle velocities in wind waves based on field measurements. *Appl. Ocean Res.*, 6: 187–196.
- Bearman, P.W., Chaplin, J.R., Graham, J.M.R., Kostense, J.K., Hall, P.F. and Klopman, G., 1985. The loading on a cylinder in post-critical flow beneath periodic and random waves. In: J. Battjes (Editor), *Proc. 4th Intl. Conf. on the Behaviour of Offshore Structures*. Elsevier, Amsterdam, pp. 213–225.
- Bendat, J.S. and Piersol, A.G., 1971. *Random data: analysis and measurement procedures*. Wiley-Interscience, New York, 407 pp.
- Cavaleri, L., Ewing, J.A. and Smith, N.D., 1978. Measurement of the pressure and velocity field below surface waves. In: A. Favre and K. Hasselmann (Eds.), *Turbulent fluxes through the sea surface, wave dynamics and prediction*. Plenum Press, New York, pp. 257–272.
- Cavaleri, L. and Zecchetto, S., 1987. Reynolds stresses under wind waves. *J. Geophys. Res.*, 92(C4): 3894–3904.
- Donelan, M.A. and Kahma, K.K., 1987. Observations of velocities beneath wind-driven waves. In: *Proc. First Intl. Workshop on Wave Hindcasting and Forecasting*, Halifax, pp. 243–252.
- Donelan, M.A. and Motycka, J., 1978. Miniature drag sphere velocity probe. *Rev. Sci. Instrum.*, 49: 298–304.
- Donelan, M.A., Anctil, F. and Doering, J.C., 1992. A simple method for calculating the velocity field beneath irregular waves. *Coastal Eng.*, 16: 399–424.
- Donelan, M.A., Hamilton, J. and Hui, W.H., 1985. Directional spectra of wind-generated waves. *Phil. Trans. Royal Soc. London A*, 315: 509–562.
- Forristall, G.Z., Ward, E.G., Cardone, V.J., and Borgmann, L.E., 1978. The directional spectra and kinematics of surface gravity waves in tropical storm Delia. *J. Phys. Oceanogr.*, 8: 888–909.
- Guza, R.T. and Thornton, E.B., 1980. Local and shoaled comparisons of sea surface elevations, pressures and velocities. *J. Geophys. Res.*, 85(C3): 1524–1530.
- Harris, F.J., 1978. On the use of windows for harmonic analysis with the discrete Fourier transform. *Proc. IEEE*, 66: 51–83.
- Jefferys, E.R., 1986. Comparison of three methods for calculation of directional spectra. In: *Proc. 5th Intl. Offshore Mechanics and Arctic Eng. Symp.*, Tokyo, Vol. 1, pp. 45–50.
- Kitaigorodskii, S.A., Donelan, M.A., Lumley, J.L. and Terray, E.A., 1983. Wave-turbulence interactions in the upper ocean. Part II: Statistical characteristics of wave and turbulent components of the random velocity field in the marine surface layer. *J. Phys. Oceanogr.*, 13: 1988–1999.
- Melville, W.K. and Rapp, R.J., 1985. Momentum flux in breaking waves. *Nature*, 317: 514–516.
- Morison, J.R., O'Brien, M.P., Johnson, J.W. and Schaaf, S.A., 1950. The force exerted by surface waves on piles. *Petroleum Trans., AIME*, 189: 149–154.
- Ramberg, S.E. and Niedzwecki, J.M., 1979. Some uncertainties and errors in wave force computations. In: *Proc. 11th Offshore Technology Conference, Houston (OTC 3597)*, pp. 2091–2101.
- Sarpkaya, T. and Isaacson, M., 1981. *Mechanics of Wave Forces on Offshore Structures*. Van Nostrand Reinhold Company, New York, 651 pp.

- Shonting, D.H., 1970. Observations of Reynolds stresses in wind waves. *Pure Appl. Geophys.*, 81: 202–210.
- Simpson, J.H., 1969. Observations of the directional characteristics of sea waves. *Geophys. J. Royal Astron. Soc.*, 17: 93–120.
- Thornton, E.B. and Krapohl, R.F., 1974. Water particle velocities measured under ocean waves. *J. Geophys. Res.*, 79: 847–852.
- Tsanis, I.K. and Donelan, M.A., 1989. Wave directional spectra in mixed seas. In: *Proc. Second Intl. Workshop on Wave Hindcasting and Forecasting, Vancouver*. Environment Canada, AES, Downsview, Ont., pp. 387–396.
- Vis, F.C., 1980. Orbital velocities in irregular waves. Report 231, Delft Hydraulics Laboratory, Delft, 13 pp.